Journal of Alloys and Compounds 488 (2009) 52–56

Contents lists available at ScienceDirect

Journal of Alloys and Compounds

journal homepage: www.elsevier.com/locate/jallcom

Phase transformation of high temperature on Fe–Al–Mn–Cr–C alloy

Chung-Ming Liu[a,b,c], Hsin-Chung Cheng[a,b], Chih-Yeh Chao[c,d], Keng-Liang Ou[c,e,*]

[a] Department of Chemical and Material Engineering, LungHwa University of Science and Technology, Taoyuan, Taiwan
[b] Graduate School of Engineering, LungHwa University of Science and Technology, Taoyuan, Taiwan
[c] Research Center for Biomedical Implants and Microsurgery Devices, Taipei Medical University, Taipei 110, Taiwan
[d] Department of Mechanical Engineering, Pingtung University of Science and Technology, PingTung 912, Taiwan
[e] Gratuate Institute of Biomedical Materials and Engineering, Taipei Medical University, Taipei 110, Taiwan

ARTICLE INFO

Article history:
Received 19 March 2009
Received in revised form 14 August 2009
Accepted 17 August 2009
Available online 25 August 2009

Keywords:
Fe–Al–Mn–C–Cr alloy
Chromium carbide
High temperature microstructure
Electron microscopy

ABSTRACT

The high temperature microstructures in the Fe–8.7Al–28.3Mn–1C–5.5Cr alloy were investigated by means of optical microscopy, electron microscopy and energy-dispersive X-ray spectrometry. When the alloy underwent heat-treatment between 800 and 1400 °C, a $(\gamma + Cr_7C_3) \rightarrow \gamma \rightarrow (\gamma + (\alpha + B2 + DO_3))$-phase transition was observed. In addition, the aluminum and chromium contents influenced the liquidus temperature of the alloy. Other researchers have not previously observed these features in the Fe–Al–Mn–C–Cr alloy system.

1. Introduction

Fe–Al–Mn–C alloys have been extensively investigated by many researchers because of their superior features, such as low density, low magnetism, high strength, high ductility, and good biocompatibility [1–7]. Hence, Fe–Al–Mn–C alloys are suitable for industrial use and in biomedical applications. The typical chemical compositions of Fe–Al–Mn–C alloys are in the ranges of Fe—(4.9–11.0) mass% Al—(23.7–35.0) mass% Mn—(0.5–1.5) mass% C [8–12]. Furthermore, it is generally concluded that Fe–Al–Mn–C alloys exhibit good oxidation resistance at high temperatures because a composition of Al between 8.5 wt.% and 10.5 wt.% results in the formation of a continuous protective Al_2O_3 layer on the surface of the alloys [13–15]. However, the corrosion resistance of Fe–Al–Mn–C alloys is inferior to that of conventional stainless steel [16]. Therefore, to increase the corrosion resistance and oxidation resistance as well as strength at high temperatures, some alloy elements such as Si, Cu, Ti, V, Nb, Mo, W and Cr, are added [17–21].

The addition of Si to Fe–Al–Mn–C alloys can significantly improve corrosion resistance [22–24]. In addition, its effects of on microstructures of austenite Fe–Al–Mn–C alloys have been extensively studied [17–19,25]. It was proposed that the addition of Si would enhance the formation of the ferrite (α)-phase in these alloys [25]. Cr was also found to be the most effective element in improving the corrosion resistance, high temperature oxidation resistance and environmental embitterment in Fe–Al–Mn alloys [26,27]. Liu's studies [16,28], indicate that increasing the amount of added Cr would expand both the A12α-Mn and DO_3-phase-field regions in the Fe–Al–Mn alloy.

However, no information concerning the addition of Cr to the Fe–Al–Mn–C alloy system has been reported. Furthermore, there are still some problems with the Fe–Al–Mn–C–Cr alloy during high temperature plastic deformation processes. Therefore, the purpose of the present study is to investigate the high temperature microstructure of the Fe–8.7Al–28.3Mn–1C–5.5Cr alloy heat-treated to 800–1400 °C.

2. Experimental procedure

The present alloy was prepared in an air induction furnace in a protective N_2 atmosphere using AISI 1008 low carbon steel, 99.7% pure electrolytic aluminum, 99.9% pure electrolytic manganese, pure carbon powder and pure chromium. The alloy was poured into a Φ40 mm × 100 mm investment casting mould that had been preheated to 1160–1180 °C. The chemical compositions of the present alloy were identified by inductively coupled plasma atomic emission spectrometry. After it was homogenized at 1200 °C for 4 h in a protective argon atmosphere, the ingot was hot-forged to a final thickness of 3.0 mm. The as-forged specimens were heat-treated at temperatures from 800 °C to 1400 °C for various periods in a vacuum furnace and then rapidly quenched in room temperature water. The surface morphologies of the specimens following treatments were analyzed by optical microscopy (OM) and scanning electron microscopy (SEM, JEOL JSM-6380). The etching solution used was 5–10% nital solution. Elemental distributions were observed using an energy-dispersive X-ray spectrometer (EDS). Electron microscopy specimens were prepared by means of a twin-jet electropolisher with an electrolyte of 60% ethanol, 30% acetic acid and 10% perchloric acid, and then examined in a JEOL-2000FX STEM operated at 200 kV.

* Corresponding author. Tel.: +886 2 27361661x5400; fax: +886 2 27395524.
E-mail address: klou@tmu.edu.tw (K.-L. Ou).

0925-8388/$ – see front matter © 2009 Elsevier B.V. All rights reserved.
doi:10.1016/j.jallcom.2009.08.072

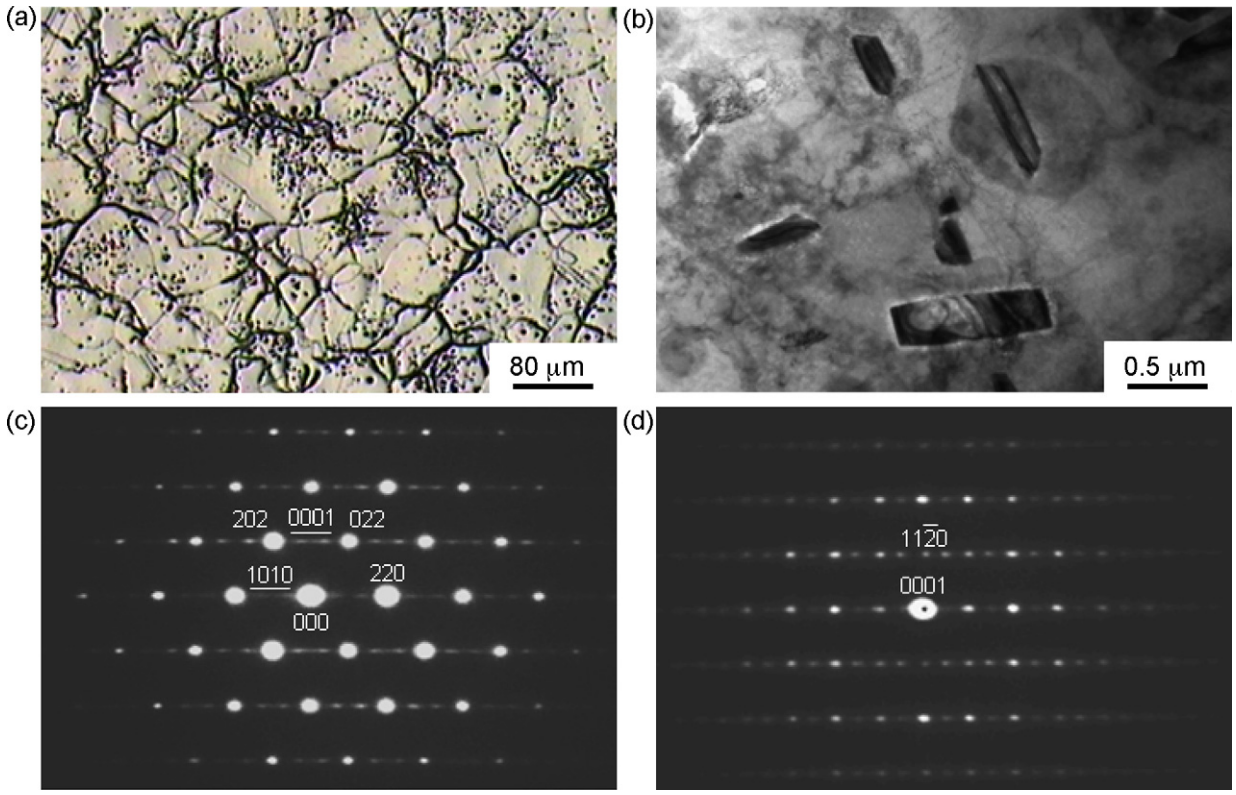

Fig. 1. Micrographs of the alloy heated at 900 °C for 30 min, (a) optical micrograph, (b–d) electron micrographs, (b) bright field (BF), (c) selected area diffraction pattern {SADP} (the foil normal is [1 1 1], hkl = austenite matrix, $\underline{hkil}$ = Cr_7C_3 − carbide) and (d) a zone axis [1 $\bar{1}$ 0 0] SADP taken from the Cr_7C_3-carbide.

3. Results and discussion

All of the as-forged specimens underwent a solution heat-treatment process to cause them to have a single austenite structure before their phase transformation was analyzed. As the alloy had undergone heat-treatment (HT) in the range 800–1000 °C, its microstructure was essentially a mixture of γ and/or (γ + precipitates) regions as shown in Fig. 1(a). These precipitates were formed within the matrix and grain boundaries. Moreover, the amounts of these precipitates increased with the HT temperature and time. Fig. 1(b) displays a bright field (BF) electron micrograph taken from the γ matrix of the alloy heat-treated at 900 °C for 30 min, indicating that some particle precipitates were formed within the γ matrix. Fig. 1(c) shows a foil normal [1 1 1] selected area diffraction pattern (SADP) taken from the γ matrix, revealing that in addition to the reflection spots of the γ-phase, the SADP also consisted of small superlattice spots. Fig. 1(d) shows a [1 $\bar{1}$ 0 0] zone axis SADP taken from the particle precipitates, suggesting that these precipitates were Cr_7C_3-phase carbide with a hexagonal structure and lattice parameters of a = 1.393 nm and c = 0.452 nm. Accordingly, when the alloy underwent HT at 800–1000 °C, its microstructure became a mixture of the γ + Cr_7C_3-carbide phases.

The microstructure of the alloy following HT at 1050–1200 °C was a single γ-phase with (1 1 1) habit plane annealing twins. Fig. 2(a) is a BF electron micrograph taken from the γ matrix of the alloy heat-treated at 1100 °C for 30 min, indicating that some dislocations were also found within the γ matrix. Fig. 2(b) shows a [1 1 0] SADP, revealing that the γ-phase has a face-center-cubic structure with the lattice parameter a = 0.380 nm. Annealing twins with a (1 1 1) habit plane were observed within the γ matrix. The twin result was similar to that reported in the Fe–Al–Mn–C alloy by other researchers [29]. No κ-phase carbides could be detected.

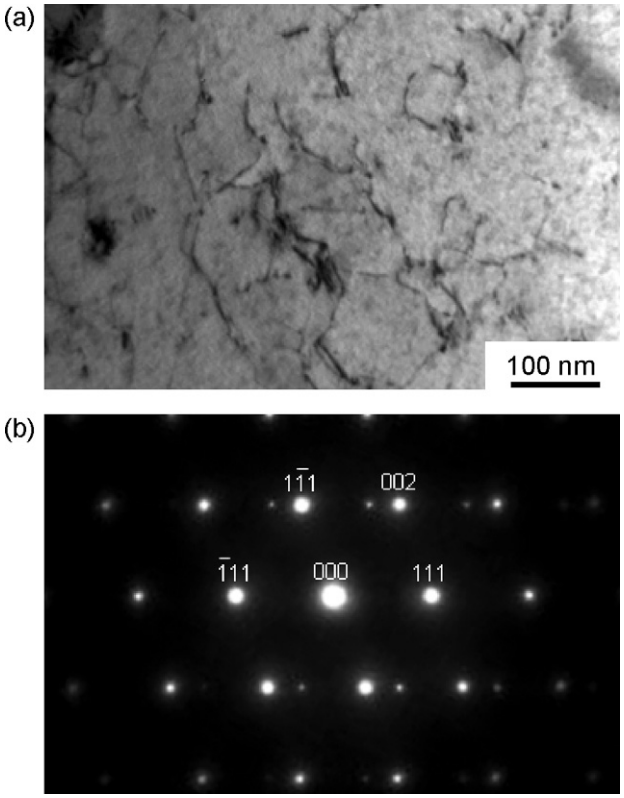

Fig. 2. Electron micrographs of the alloy heated at 1100 °C for 30 min, (a) BF and (b) a zone axis [1 1 0] SADP taken from the austenite matrix.

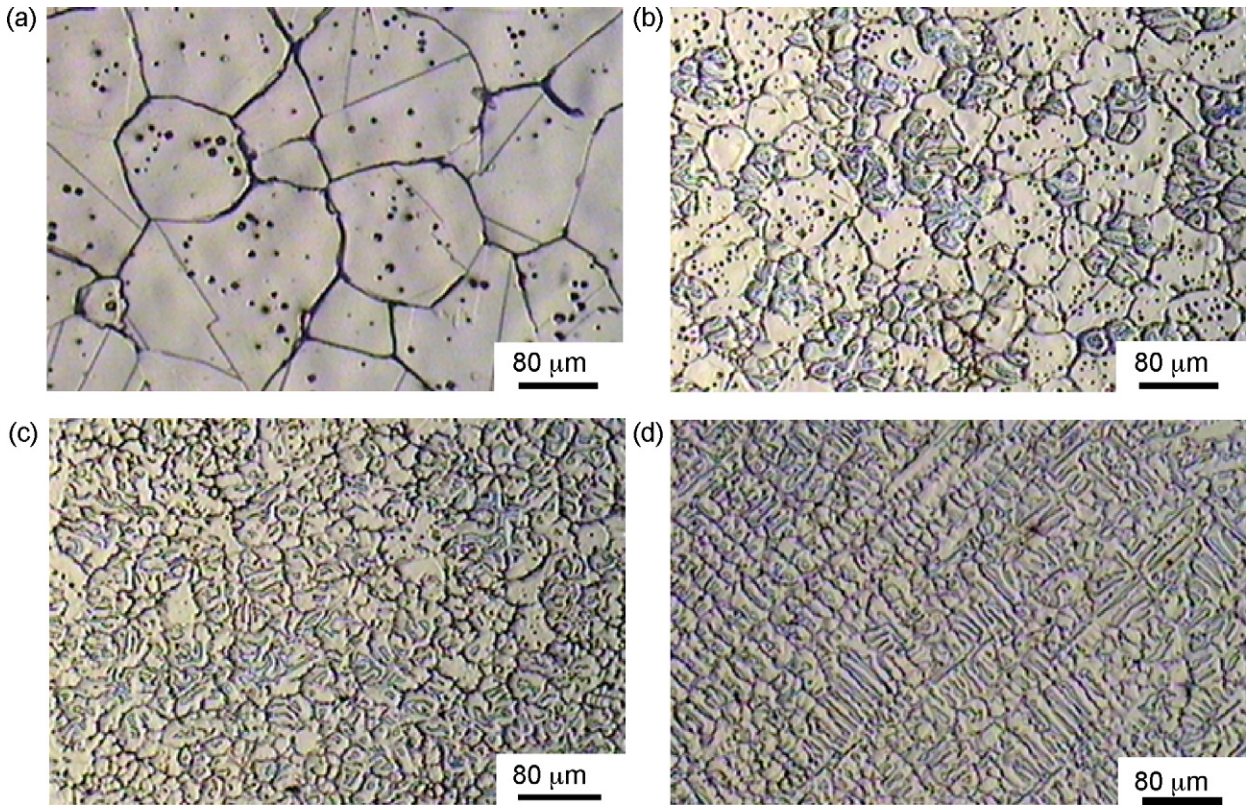

Fig. 3. Optical micrographs of the alloy heated at (a) 1250 °C, (b) 1300 °C, (c) 1350 °C, and (d) 1400 °C for 5 min.

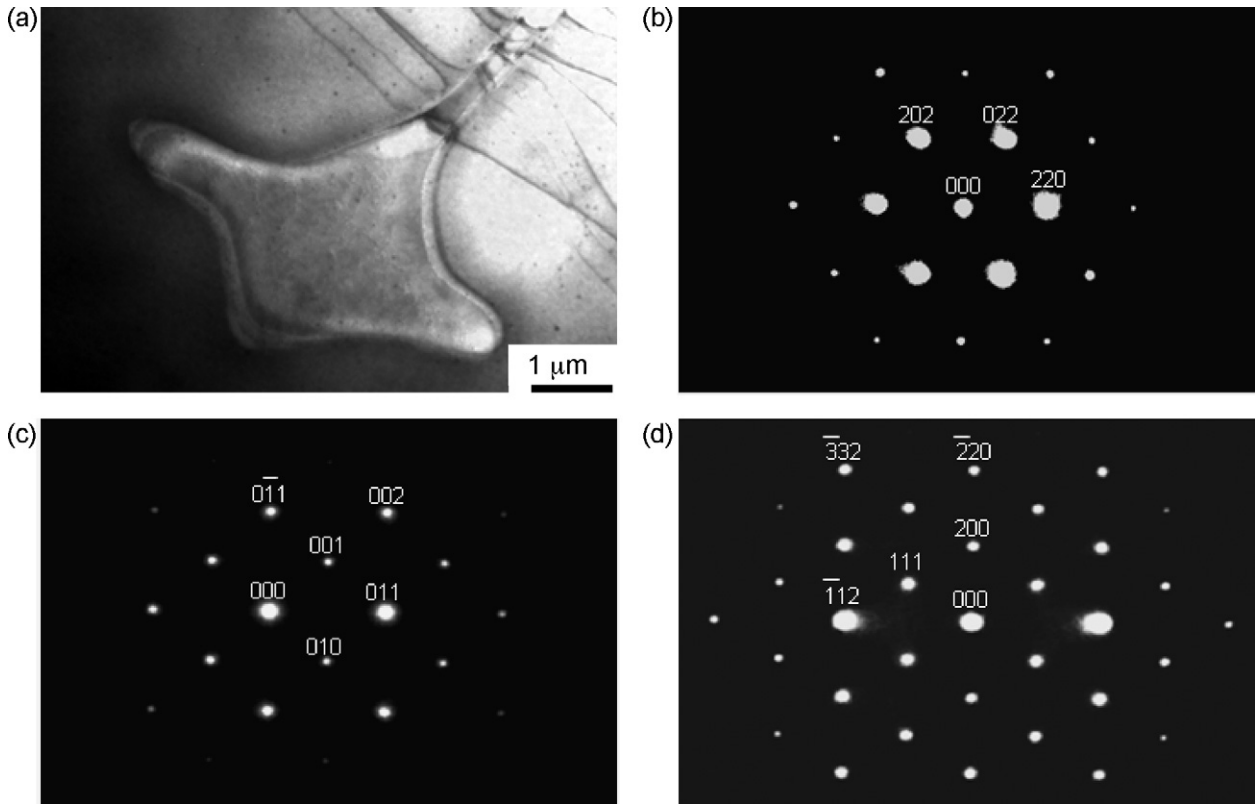

Fig. 4. Electron micrographs of the alloy heated at 1300 °C for 5 min, (a) BF, (b) a zone axis [1 1 1] SADP taken from the RS region, (c) and (d) foil normal [1 0 0] and [1 1 0] SADPs, respectively, taken from the DO_3-phase.

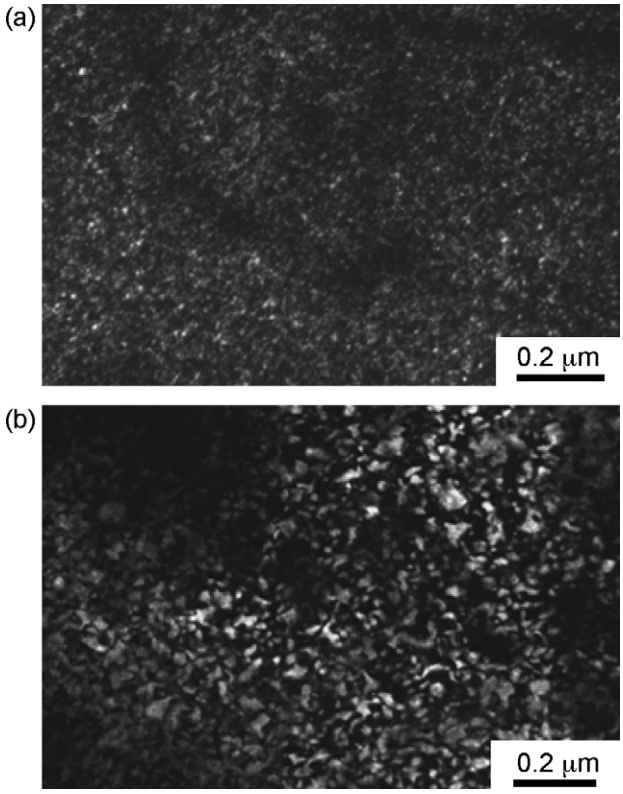

Fig. 5. Electron micrographs taken from the DO_3-phase of the alloy heated at 1300 °C for 5 min, (a) (1 1 1) DO_3 DF, and (b) (2 0 0) DO_3 DF.

After increasing the HT temperature to between 1250 °C and 1400 °C for 5 min, some re-solidified (RS) regions were formed within the γ matrix and grain boundaries as illustrated in Fig. 3. In addition, the sizes of the RS regions increased with the HT temperature. Fig. 4(a) shows a BF electron micrograph taken from the γ matrix of the alloy heat-treated at 1300 °C for 5 min, revealing that a RS region was formed at the grain boundaries. Fig. 4(b–d) shows foil normal [1 1 1], [1 0 0] and [1 1 0] SADPs, respectively, taken from the RS region. Fig. 4(b) indicates that the RS region is ferrite (α)-phase which has a body-center-cubic structure. In addition, Fig. 4(c) and (d) also reveal that the DO_3-phase consists of the α-phase, with the DO_3-phase lattice parameter $a = 0.565$ nm. Furthermore, according to previous studies [30–32], (2 0 0) DO_3 reflections overlap with (1 0 0) B2 reflections, so the (2 0 0) DO_3 dark field (DF) images were possibly also derived from the B2 superlattice. If this situation occurred, the B2 domains shown in the DF electron micrograph of (2 0 0) DO_3 reflections would be expected to be somewhat larger than the DO_3 domains shown in that of the (1 1 1) DO_3 reflections for the continuous ordering transition. Fig. 5(a) and (b) shows $\vec{g} = 1\,1\,1$ and $\vec{g} = 2\,0\,0$ DF electron micrographs, respectively, taken from the DO_3 region. It is clearly seen in Fig. 5(b) that the (2 0 0) DO_3 is somewhat larger than that observed in the (1 1 1) DO_3 shown in Fig. 5(a). Hence, it could be proved that the B2 structure was observed in this study. This result was the same as that observed by other research with the Fe–Al alloy [33], Fe–Al–Mn–C alloy [31] and Fe–Al–Mn–C–Si alloy system [34,25]. But, other researchers have not observed these results at this temperature range in the Fe–Al–Mn–C–Cr alloy system. Basically, when the temperature was increased to 1400 °C, the microstructure of the alloy was dendritic as shown in Fig. 3(d). Therefore, in this temperature range, the microstructure in the present alloy was a mixture of the γ + (α + B2 + DO_3)-phases.

In the Fe–Al–Mn alloy system, it is well known that Mn and Al are austenite and ferrite formers, respectively [30]. An amount of Al above 6.5 wt.% results in the formation of a continuous protective Al_2O_3 layer on the surface of Fe–Al–Mn alloys. Thus, the corrosion and oxidation resistance characteristics can be improved. However, if the amount of Al is over 10.5 wt.%, an $\alpha \rightarrow \alpha + B2(FeAl) \rightarrow \alpha + DO_3(Fe_3Al)$ ordering transition will occur. The B2-phase results in embitterment of the Fe–Al–Mn alloy system [13–15,35]. Based on the above results, when the alloy underwent HT at 1300 °C, some RS regions were formed within the matrix and at the grain boundaries. It can be deduced that this occurred because the melting point of the Al element was lower than that of other elements in the alloy. Hence, the Al element diffused and/or segregated at this high temperature. In order to clarify this deduction, an SEM-EDS study was undertaken. The average atomic percentages of alloying elements were examined by analyzing at least five different EDS spectra of each phase, as listed in Table 1. It was clearly demonstrated that the Al and Cr contents in the RS region exceeded those in the γ matrix. Accordingly, the RS regions were formed on the grain boundaries because of the Al diffusion and/or segregation of the alloy that underwent HT at 1300 °C. In addition, the Cr content in the RS region exceeded that in the γ matrix, suggesting that the Al and Cr contents influenced the liquidus temperature in the alloy. The liquidus temperature of the Fe–8.7Al–28.3Mn–1C–5.5Cr alloy was around 1300 °C. Furthermore, the Al content within the RS region was about 10.5 wt.% as shown in Table 1. Therefore, it is reasonable that when the present alloy underwent SHT at 1300 °C, the (α + B2 + DO_3)-phases were observed within the RS regions.

Table 1
Chemical compositions of the phases revealed by an energy-dispersive spectrometer (EDS).

		Chemical composition (wt.%)				
Heat-treatment	Phase	Fe	Al	Mn	C	Cr
1300 °C/5 min	γ-phase	Bal.	8.53	28.16	0.83	3.82
	(α + B2 + DO_3)-phase	Bal.	10.51	27.03	0.12	6.03

4. Conclusions

When the present alloy underwent HT between 800 °C and 1000 °C, the microstructure of the alloy was a mixture of (γ + Cr_7C_3)-phases. The Cr_7C_3-phase carbide had a hexagonal structure and lattice parameters of $a = 1.393$ nm and $c = 0.452$ nm.

The microstructure of the alloy following HT at 1050–1200 °C was a single γ-phase with (1 1 1) habit plane annealing twins. The γ-phase has a face-center-cubic structure with the lattice parameter $a = 0.380$ nm. No κ-phase carbides could be detected.

After increasing the HT at temperatures ranging from 1250 °C to 1400 °C, the microstructure of the alloy was a mixture of the γ + (α + B2 + DO_3)-phases. The lattice parameter of the DO_3-phase was $a = 0.585$ nm.

RS regions were formed on the grain boundaries because of the Al diffusion and/or segregation of the alloy that underwent HT at 1300 °C. In addition, the Cr content in the RS regions exceeded that in the γ matrix, suggesting that the Al and Cr contents influenced the liquidus temperature in the present alloy.

Acknowledgments

The authors would like to thank the National Science Council of Republic of China for financially supporting this research under Contract No. NSC95-2314-B-038-032, Center of Excellence for Clinical Trial and Research in Neurology and Neurosurgery financially supporting this research under contract No. DOH-TD-B-111-002, and supported partly by Taipei Medical University Hospital under contract 96TMU-TMUH-13.

References

[1] P.J. James, J. Iron Steel Inst. 54 (1969).
[2] P.R. Rao, V.V. Kutumbarao, Int. Mater. Rev. 34 (2) (1989) 69.
[3] I.S. Kalashnikova, Phys. Met. Metallogr. 57 (1984) 160.
[4] Y.G. Kim, Y.S. Park, J.K. Ham, Metall. Trans. A 16 (1985) 1689.
[5] Y.G. Kim, J.K. Ham, E.W. Lee, Metall. Trans. A 17 (1986) 2097.
[6] S.L. Chen, M.H. Lin, C.C. Chen, K.L. Ou, J. Allo. Compd. 456 (2008) 413.
[7] C.Y. Chao, C.H. Liu, Mater. Trans. 43 (10) (2002) 2635.
[8] C.C. Wu, J.S. Chou, T.F. Liu, Metall. Trans. A 22A (1991) 2265.
[9] C.Y. Chao, T.F. Liu, Scripta Metall. 25 (1991) 1623.
[10] T.F. Liu, J.S. Chou, C.C. Wu, Metall. Trans. A 21A (1990) 1891.
[11] J.C. Benz, H.W. Leavenworth Jr., J. Met. 36 (1985), March.
[12] J.E. Krzanowski, Metall. Trans. A 19A (1988) 1873.
[13] Z. Sun, H.A. Davies, J.A. Whiteman, Met. Sci. 18 (1984) 45.
[14] A. Inoue, Y. Kojima, T. Minemura, T. Masumoto, Metall. Trans. A 12A (1982) 1245.
[15] S.C. Chan, Y.H. Hsian, J. Mater. Sci. 24 (1989) 1117.
[16] J.W. Lee, C.C. Wu, T.F. Liu, Scripta Mater. 50 (2004) 1389.
[17] K.H. Han, W.K. Choo, Metall. Trans. A 14A (1983) 973.
[18] K.G. Kim, Y.S. Park, J.K. Han, Metall. Trans. A 16A (1985) 1689.
[19] K.H. Han, W.K. choo, D.E. Laughlin, Scripta Metall. 22 (1988) 1873.
[20] K. Sato, K. tagawa, Y. Inoue, Mater. Sci. Eng. A111 (1989) 45.
[21] N.A. Storchak, A.G. Drachinskaya, Phys. Met. Metallogr. 44 (1977) 123.
[22] R. Wang, F.H. Beck, Met. Prog. (1983) 72, March.
[23] U. Bernabai, G.A. Capuano, A. Dang, F. Felli, Oxid. Met. 33 (1990) 809.
[24] J.P. Sauer, R.A. Rapp, J.P. Hirth, Oxid. Met. 18 (1982) 285.
[25] J.W. Lee, T.F. Liu, Mater. Chem. Phys. 69 (2001) 192.
[26] T.F. Liu, C.M. Wan, Scripta Metall. 23 (1989) 1243.
[27] R. Wittmann, S. Spindler, B. Fischer, H. Wagner, D.J. Gerthsen, Mater. Sci. 34 (1999) 1791.
[28] T.F. Liu, C.M. Wan, Scripta Metall. 23 (7) (1989) 1087.
[29] W.C. Cheng, H.Y. Lin, Mater. Sci. Eng. A 341 (2003) 106.
[30] W.C. Cheng, C.F. Liu, Y.F. Lai, Mater. Sci. Eng. A 337 (2002) 281.
[31] Y.L. Lin, C.P. Chou, Scripta Metall. 28 (1993) 1261.
[32] S.M. Allen, J.W. Cahn, Acta Metall. 24 (1976) 425.
[33] G. Frommeyer, H.J. Habrock, J.E. Wittig, J. Geenen, M. Kreuss, Scripta Metall. 24 (1990) 51.
[34] J.C. Garcia, N. Rosas, R.J. Rioja, Met. Prog. (1982) 47, August.
[35] K.H. Han, W.K. Choo, Metall. Mater. Trans. A 20 (1989) 205.